Cosmic Ray phenomenology and measurement of the σ_{p-Air} with the ARGO-YBJ Experiment

A. Surdo[a] for the ARGO-YBJ Collaboration
([a]) INFN - Sezione di Lecce, via Arnesano, 73100 Lecce, Italy
Email: surdo@le.infn.it

Abstract— **The ARGO-YBJ experiment is currently operating at the high altitude Cosmic Ray Laboratory of Yangbajing (Tibet, P.R.China, $4300\ ma.s.l.$), with about $5600\ m^2$ of detector in data taking. One of the major aims of ARGO-YBJ is the study of cosmic ray physics below the knee of the primary spectrum, by exploiting the full coverage technique and the high space-time granularity of the detector. In this work the detector performance in the shower reconstruction and the first results of data analysis for the study of cosmic ray phenomenology will be presented. In particular, the preliminary measurement of the inelastic $p - Air$ cross section together with a first estimation of the total σ_{p-p} above $E_p \sim 1\ TeV$ will be discussed.**

I. Introduction

As a result of a collaboration between INFN (Italy) and Chinese Academy of Science, the ARGO-YBJ (Astrophysical Radiation with Ground-based Observatory at YangBaJing) experiment [1] will exploit the full coverage technique and the high altitude operation in order to deeply investigate cosmic radiation physics. In more details, through the observation at high altitude of Extensive Air Showers (EASs) produced in the atmosphere by primary photons and nuclei, ARGO-YBJ will inspect a wide range of fundamental issues in cosmic ray and astroparticle physics:

- very high energy γ-ray astronomy, with an energy threshold of a few hundreds GeV;
- search for emission from gamma ray bursts in the full $GeV - TeV$ energy range;
- study of cosmic rays (spectrum, composition, anti-p/p ratio measurement, shower space-time structure, ...) starting at TeV energies;
- Sun and heliosphere physics above $E_{thresh} \sim 1\ GeV$.

The detector is being installed at the Yangbajing High Altitude Cosmic Ray Laboratory ($4300\ m\ a.s.l.$, $606\ g/cm^2$), 90 km North of Lhasa (Tibet, P.R.China), and is currently near its final configuration. It consists of a single layer of Resistive Plate Counters (RPCs), with dimension $74 \times 78\ m^2$. The apparatus performance in detecting showers with core outside the full coverage carpet will be improved by partially instrumenting the area surrounding the central detector with a guard ring of RPCs, up to $\sim 100 \times 110\ m^2$. Moreover, a $0.5\ cm$ thick lead converter will cover uniformly the RPCs plane to increase the number of charged particles by conversion of shower photons and to reduce the shower front time spread.

The site location (longitude $90^\circ\ 31'\ 50''\ E$, latitude $30^\circ\ 06'\ 38''\ N$) will allow the monitoring of the sky in the declination band $-20^\circ < \delta < 80^\circ$.

In a logical subdivision of the apparatus, the basic detection and Data Acquisition unit is the 'Cluster' (area = $5.7 \times 7.6\ m^2$), made of 12 RPCs, each RPC being of dimension $280 \times 125\ cm^2$ [2]. The percentage of active area in the central detector, made of 130 Clusters, is $\sim 92\%$.

The whole full coverage central carpet ($\sim 5600\ m^2$) is in smooth data taking since August. In the meantime the external guard ring began to be instrumented and will be included in the DAQ system by the end of this year. In order to fully investigate the above listed physics items, a 'scaler mode' as well as a 'shower mode' trigger for cosmic rays detection is implemented.

Since December 2004, two phases of data taking with a portion of the detector took place both for debugging the apparatus and for studying its performance: (1) 42 clusters ($\sim 1800\ m^2$ of active area) were in data acquisition for a total live time of $\sim$ 3 months in the first half of 2005; (2) during the first half of the current year, several runs were performed on 104 clusters ($\sim 4500\ m^2$ of active area). This work will mainly discuss the performance and potentialities of the ARGO-YBJ detector in atmospheric shower physics and will focus on some preliminary results of the 42 Clusters data analysis concerning the very high energy cosmic rays interactions.

II. Detector features and performance

The capability of an EAS detector in sampling and reconstructing the shower front of atmospheric cascades is primarily determined by its intrinsic time resolution and space-time granularity. In ARGO-YBJ every detecting element (the RPC) is segmented into 10 'pads' ($56 \times 62\ cm^2$), each one composed by 8 'strips' ($6.7 \times 62\ cm^2$) for the pick-up of the single charged particles signals. The space information is thus provided by the strip, while the pad signal ('Fast-OR' of 8 strips) is used for timing (defining the 'time granularity' of the detector) and for trigger purposes. The pad Fast-OR signals sent to TDCs are shaped to $90\ ns$, thus we are able to detect also 'multiple hits', that is the times of several particles hitting the same pad with a $90\ ns$ time delay can be recorded. The intrinsic time resolution of the RPCs is $\sim 1\ ns$.

Such characteristics (together with the full coverage of a large area and the high altitude operation) of ARGO-YBJ ensure a pointing accuracy better than 0.5° with a few hundreds of hits, as well as the capability of detecting small (that is low energy) showers and a detailed space-time imaging of the shower front. Finally, the large field of view ($> \pi\ sr$)

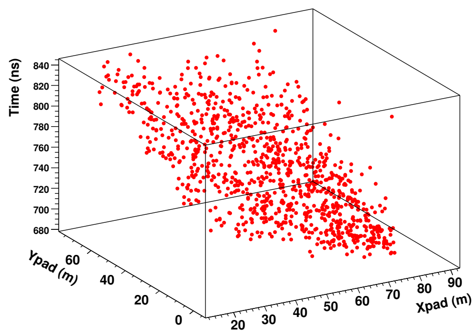

Fig. 1. Space-time picture of a shower event detected by ARGO-104.

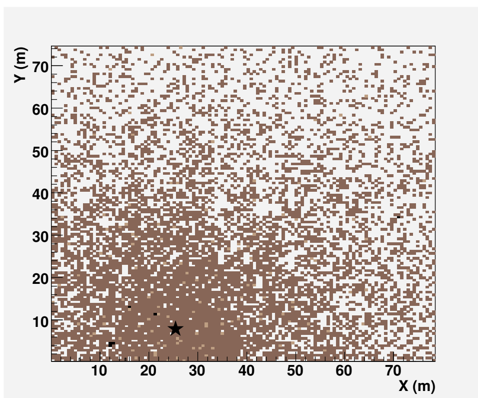

Fig. 2. X-Y pattern (at pad level) of a very large shower detected by ARGO-130, useful for topological structure studies. The reconstructed core is represented by a star in the picture.

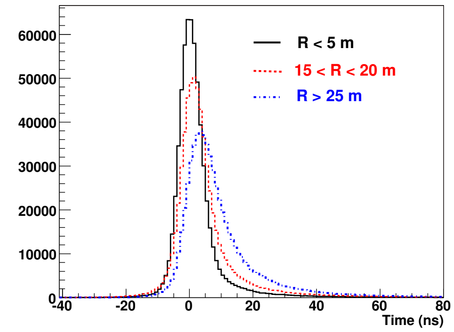

Fig. 3. Shower time profile for different intervals of the hit distance R from the reconstructed core.

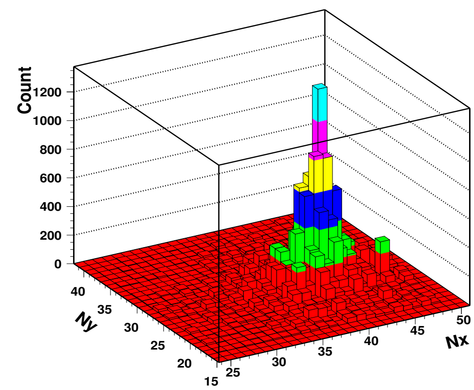

Fig. 4. Charge density profile of one event as reconstructed by means of the analog read-out set-up. The charge peak correspond to about 3500 particles.

and the possibility of a high duty-cycle ($\sim 100\%$) will allow a continuous monitoring of the sky in a wide declination range.

Fig. 1 shows an example of a shower event detected by 'ARGO-104 Clusters' (ARGO-104). This figure allows to point out how that peculiar features give ARGO-YBJ a unique way to deeply investigate the structure and lateral development of EASs, by means of a full space-time reconstruction and the study of the topological structure and time profile of the shower front.

Fig. 2 provides the image (like a pure space pattern) of a very large shower, most probably initiated by a several TeV primary, detected by the whole ARGO-YBJ central carpet (ARGO-130). For this kind of shower events, whose core is well reconstructed inside the active detector area, both the lateral hit density profile and the time width of the shower front (as reported in Fig. 3) can be precisely measured at different distances from the core position.

Moreover, for such very energetic shower events saturating the digital strip information, the read-out of the analog charge released in the RPCs is also provided, on the basis of a local high multiplicity trigger. The analog charge information from a 'big-pad' large one half of the RPC area is then digitized and included in the normal event data stream. Fig. 4 is an example of the events as seen by the analog read-out set-up, where the highest charge peak corresponds to about 3500 particles intercepting one big-pad (~ 2000 charged particles $/m^2$).

Such a capability of imaging and inspecting the showers structures in so many details could in principle be exploited to give some hints for discriminating between hadron and gamma-initiated cosmic ray showers. This possibility is currently being investigated in our collaboration.

Considering the opposite extreme, ARGO-YBJ is able to detect spatially concentrated (although not so poor) showers, like that shown in Fig. 5, probably induced by primary protons interacting in the atmosphere only a few radiation lengths above the detector. Here a conical shape of the front is rather evident, while several tens or hundreds of hits are concentrated in spots of a few meter dimensions thus suggesting quite high local charge densities.

The examples reported are enough to provide an idea of the large variety and possibly unexpected phenomenology of EASs that ARGO-YBJ is able to deeply investigate.

III. Shower Event Reconstruction

The reconstruction of the shower arrival direction is obtained from the time profile of the shower front, that is the relative arrival times of the shower particles. Thus its accuracy essentially depends on the precision of the time information provided by each fired pad on the detector.

The time resolution of each pad is the result of: the RPC intrinsic resolution, the propagation of the signal along the

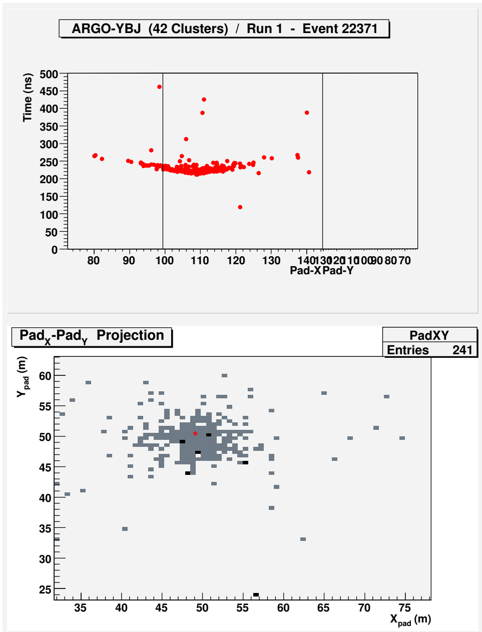

Fig. 5. Picture of a spatially concentrated event (the darker dots indicate the pads with multiple time-hits). A conical shape in the time profile of the shower front can be appreciated.

strip (62 cm) and the electronic time resolution. An additional factor arises from the timing offset between different read-out channels due to variations in the discharge time of the RPCs, different cable delays and other instrumental effects. So, as a preliminary step, a 'detector time calibration', that is a correction for the relative time offset among different pads, must be performed.

For particles not far from the core (within a few tens of meters), the shower front shape is expected to appear conical.

The procedure used to reconstruct the arrival direction of the shower has 2 steps: (1) times and positions of all the pad hits in the event are fitted to a plane by a χ^2 minimization; (2) fit of the same space-time coordinates to a cone, by adding a correction $\alpha \cdot R_i/c$, where R_i is the distance of the i-th pad from the reconstructed core in the plane determined in step (1) and $\alpha/c = 0.03\ ns/m$.

Both steps can be iterated several times, rejecting after each cycle the outlying times by means of a $k\ \sigma$ cut (σ being the standard deviation of the time distribution around the fitted front and $k = 2.5$ in this analysis). The procedure is rather fast, because both fits make use only of analytical formulas. In order to fit the shower particles to a conical shape, the position of the core is needed and several algorithms have been implemented in ARGO-YBJ for reconstructing it.

The direction reconstruction performance of the detector, obtained for several configurations, is discussed in a separate contribution to these Proceedings [3].

The differential density spectrum of EASs allows to obtain information on the size spectrum, since both spectra follow a power law with close indexes. Fig. 6 shows the density spectrum for three intervals of zenith angle: the shapes of

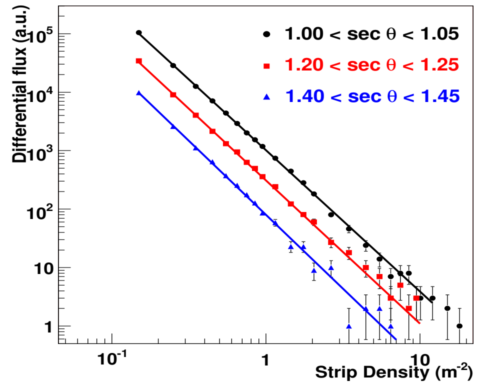

Fig. 6. Differential strip density spectra measured for different intervals of zenith angle.

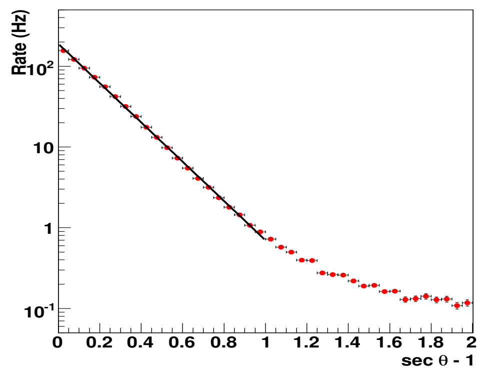

Fig. 7. Zenith angle distribution of detected showers. It can be well fitted out by an exponential up to about 60^o.

the spectra are very similar and the average index is $\beta = -2.38$. This result agrees with our expectation, because the integral density spectrum changes very slowly with altitude and particle density.

The zenith angle distribution of events with particle density exceeding a given value is expected to follow an exponential behaviour $I(\geq\ \rho,\theta)\ =\ I(\geq\ \rho,0)\ e^{-x_0/\Lambda_{att}(sec\theta-1)}$, where x_0 is the vertical depth and Λ_{att} is the attenuation length of showers with particle density exceeding ρ. The validity of this behaviour extends over an angular range where the atmospheric overburden increases as $1/cos\theta$. Fig. 7 reports the angular distribution as obtained from the events detected by ARGO-42: the data can be fitted up to $\sim 60^\circ$ by means of an $e^{-\alpha\ (sec\theta-1)}$ law, with $\alpha \equiv x_0/\Lambda_{att} = 5.61 \pm 0.11$. As a consequence, since at the Yangbajing altitude $x_0 = 606\ g/cm^2$, we obtain $\Lambda_{att}\ =\ (108 \pm 2)\ g/cm^2$. The deviation from this law at angles $> 60^\circ$ is mainly due to misreconstructed events and horizontal air showers mainly produced by muon bremsstrahlung deep in the atmosphere.

The study of the hit (pad and strip) size spectrum, of the hit density distribution, of the lateral hit and charge profiles, of the zenith angle distribution and so on, can be useful to obtain information on several important items of cosmic rays

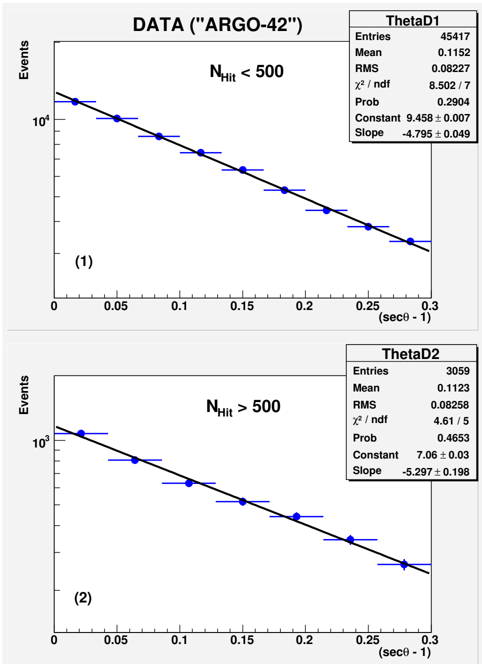

Fig. 8. Experimental zenith angle distributions for the two event sub-samples obtained by means of the N_{Hit} cut: (1) for $N_{Hit} < 500$, (2) for $N_{Hit} > 500$. The observed absorption lengths obtained from the fit slopes are reported in the text.

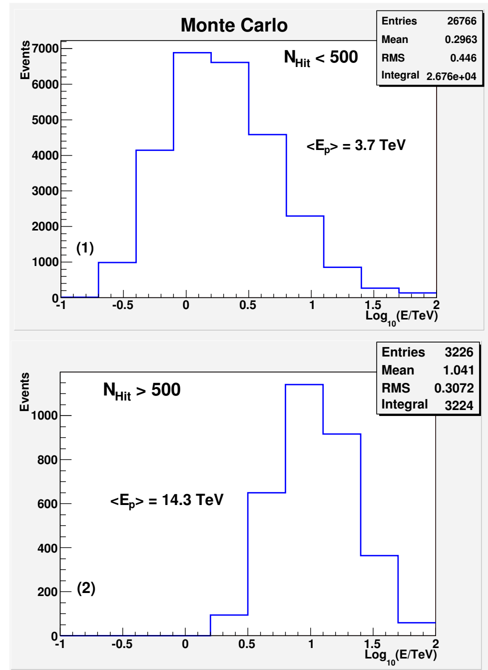

Fig. 9. Energy distributions for the two Monte Carlo event sub-samples obtained through the same analysis cuts of real data. The mean energies are $E_1 = (3.67 \pm 0.04)\ TeV$ and $E_2 = (14.3 \pm 0.2)\ TeV$, respectively.

physics, like for instance: energy spectrum (see [4]), chemical composition, hadronic cross section at very high energies. The results of a very preliminary analysis on the last item, using a reduced data sample collected with ARGO-42, will be presented and discussed in the followin section.

IV. Measurement of inelastic σ_{p-Air} and first estimation of total σ_{p-p}

The shower frequency as a function of zenith angle like that in Fig. 7, when considered at a certain primary energy (and possibly at a fixed shower age) gives a measure of the flux attenuation at that energy. Such a flux attenuation is ruled by the absorption length Λ which is related to the interaction length (or mean free path) λ_{int} of the EAS primary for collisions with air nuclei, through the parameter κ: $\Lambda = \kappa \cdot \lambda_{int}$. Thus, in principle, from Λ we can infer an estimation of $p - Air$ and $p - p$ cross sections[1]. The simple factor κ is introduced to take into account the effects of the intrinsic fluctuations in the shower development through the atmosphere. It must be evaluated by Monte Carlo (MC) simulations, so it depends on the features of the adopted hadronic interaction model as well as on the detector response.

Such a measure was also made in other cosmic ray experiments (for instance 'Akeno' and 'Fly's Eye') at extremely

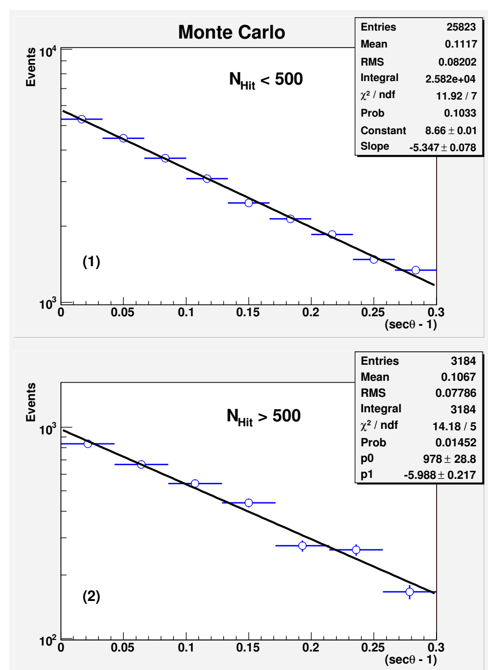

Fig. 10. Monte Carlo zenith angle distributions for the two event sub-samples obtained through the same analysis chain as for real data: (1) for $N_{Hit} < 500$, (2) for $N_{Hit} > 500$. The MC 'observed' absorption lengths obtained from the fit slopes are used to determine the parameters κ_1 and κ_2, which will be applied as correction factors to the experimental absorption lengths (see text).

[1]As well known, the primary cosmic ray flux is not purely constituted by protons, but also includes heavier nuclei which tend to make Λ smaller. However, in this preliminary analysis we assume that, in the ARGO-YBJ energy region here considered, the contribution of heavier nuclei is not relevant in determining the Λ value. In fact, the estimation of the contribution by Helium is currently in progress through a Monte Carlo simulation.

high energies, not accessible by ARGO-YBJ. They used well known techniques, but not free of criticisms, based on the measurement of N_e, N_μ and X_{max} of detected showers. The approach used in this analysis for the ARGO-YBJ data is quite different: the event selection is based on N_{Hit} (the shower size measured on the detector), together with some constraints on the reconstructed core position (forced in a fixed area inside the detector) and on the shower density profile and spatial extension. The hit multiplicity is simply used to split the data set in two sub-samples of showers quite separate in energy. To obtain this, a cut value $N_{hit} = 500$ has been chosen. Fig. 8 shows the experimental event distributions as a function of $sec\ \theta_{zenith}$ (or atmospheric depth) for the two shower sub-samples. The fit to these distributions with an exponential law gives the slope value α, connected to the absorption length Λ through the relation $\Lambda = x_0/\alpha$, where $x_0 = 606\ g/cm^2$. Thus we obtain the observed (real data) absorption lengths $\Lambda_1^{DATA} = (126 \pm 1)\ g/cm^2$ and $\Lambda_2^{DATA} = (114 \pm 4)\ g/cm^2$.

A full MC simulation, including proton-initiated showers produced with Corsika [5], the complete detector simulation, the trigger and analysis chain as for real data, allows to estimate the mean primary energy for the two shower sub-samples (Fig. 9) as well as the ‘observed’ MC absorption lengths: Λ_1^{MC} and Λ_2^{MC} (Fig. 10). From these lengths we obtain the two correction factors, κ_1 and κ_2, by using the formula $\kappa_i = (1/2.4 \cdot 10^4) \cdot \Lambda_i^{MC} \cdot \sigma_{p-Air}$, where σ_{p-Air} (in mb) is the inelastic p-Air cross section of the ‘QGSJET model’ used in the MC simulation, for the two estimated mean energy values, and Λ_i^{MC} is expressed in g/cm^2. In general, the correction parameter κ gives a measure of how the intrinsic fluctuations in the shower development through the atmosphere affect our observables and it is important to check if its value changes when a different interaction model is used in the MC simulation. Such a test of adopting a different interaction model in the simulation is currently under way.

Using the correction parameters κ_1 and κ_2, we then obtain the measured σ_{p-Air} for the two energy values: $\sigma_{p-Air}^{(1)} = (273 \pm 15)\ mb$ at $E_p = 3.67\ TeV$ and $\sigma_{p-Air}^{(2)} = (289 \pm 20)\ mb$ at $E_p = 14.3\ TeV$. The results are reported in Fig. 11 and, although to be considered as very preliminary, they appear in fair agreement with other existing measurements.

Finally, from the inelastic σ_{p-Air}, the total $p-p$ cross section can be derived using several current models [6]. These models agree within $\sim 5\%$ in our energy range, thus we introduce an additional 5% of systematic uncertainty to the mean value obtained for the total σ_{p-p} with our data. Such a very preliminary estimation of the total σ_{p-p} is shown in Fig. 12: $\sigma_{pp}^{(1)} = (39 \pm 4)\ mb$ and $\sigma_{pp}^{(1)} = (44 \pm 5)\ mb$ for the two energy values, respectively. Again our results are in good agreement with the extrapolation of other measurements to the ARGO-YBJ energy region.

V. Conclusion

ARGO-YBJ is almost completed, with $\sim 5600\ m^2$ of detector area now in data taking. The analysis of the data collected with a portion of the final apparatus shows a good performance in shower reconstruction and pointing accuracy, although further improvements are possible. Moreover, first interesting results were obtained from ARGO-42 data analysis in cosmic ray physics, in particular the preliminary measurement of the very high energy inelastic σ_{p-Air} and total σ_{p-p}. We point out that this analysis should only be considered as a test of applicability to the ARGO-YBJ experiment. However, the results we obtained suggest a promising extension to unexplored energy regions, thanks to the digital information of the strips and, mostly, to the analog charge read-out.

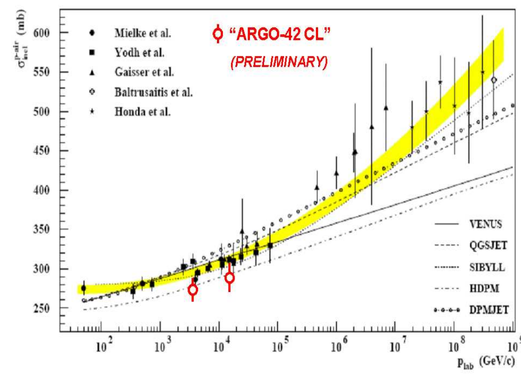

Fig. 11. Inelastic $p-Air$ cross section preliminarily measured with a data sample of ARGO-42 (open circles), compared to other measurements and theoretical estimations.

Fig. 12. Preliminary ARGO-42 measurement of the total $p-p$ cross section (open circles), compared to other existing experimental values. The error bars include both statistical and systematical uncertainties.

References

[1] M. Abbrescia et al. (ARGO-YBJ Coll.), *Astroparticle Physics with ARGO*, Proposal (available at http://argo.na.infn.it), 1996.

[2] G. Aielli et al. (ARGO-YBJ Coll.), *Nucl. Inst. and Meth. in Phys. Res. A*, vol.562, p.92, 2006.

[3] G. Di Sciascio et al. (ARGO-YBJ Coll.), *Measurement of the angular resolution of the ARGO-YBJ detector*, these Proceedings.

[4] L. Saggese et al. (ARGO-YBJ Coll.), *Measurement of strip size spectrum with the ARGO-YBJ experiment)*, 29th ICRC - Pune, India, 2005.

[5] J. Knapp and D. Heck, *Extensive Air Shower Simulation with CORSIKA (6.203)*, 1998.

[6] R.J. Glauber and G. Matthiae, *Nucl. Phys. B*, vol.21, p.135, 1970; L. Durand and H. Pi, *Phys. Rev D*, vol.38, p.78, 1988; T. Wibig and D. Sobczynska, *J. Phys. G: Nucl. Part. Phys.*, vol.24, p.2037, 1998.